ChemComm

FEATURE ARTICLE

View Article Online
View Journal | View Issue

Cite this: *Chem. Commun.*, 2025, **61**, 2011

Green solvent strategies for the sustainable development of perovskite solar cells

David Sunghwan Lee, † Hyong Joon Lee, † Yunmi Song, Jin Kyoung Park, Jin Hyuck Heo * and Sang Hyuk Im *

Received 14th October 2024,
Accepted 17th December 2024

DOI: 10.1039/d4cc05454g

rsc.li/chemcomm

Perovskite solar cells have been of great interest over the past decade, reaching a remarkable power conversion efficiency of 26.7%, which is comparable to best performing silicon devices. Moreover, the capability of perovskite solar cells to be solution-processed at low cost makes them an ideal candidate for future photovoltaic systems that could replace expensive silicon and III–V systems. However, the current state of solution-processing of perovskite solar cells is heavily dependent on toxic solvents such as DMF, chlorobenzene, diethyl ether and so on. As perovskite devices approach commercialization and large-scale fabrication, a solution must first be found to reduce the toxic risks associated with the processes. This review article presents a summary of general attempts at achieving fully green-processed perovskite solar cell fabrication. A thorough examination of popular solvents and possible alternatives is first performed, followed by their applications in perovskite layer fabrication (including solvents and anti-solvents) and charge transport layer fabrication processes.

1. Introduction

Throughout the 21st century, mankind has become more aware of lurking dangers of climate change due to increased carbon emission, and thus, in retaliation, world leaders have set out long-term goals at the Paris Agreement of 2015, notably aiming to reach net-zero carbon emission by the year 2050.[1] By recognizing fossil fuels as the largest source of carbon emission, scientists have been rigorously searching for clean energy sources that are not only carbon-free but also able to meet the global energy demand to replace fossil fuel, including but not limited to geothermal, nuclear and renewable sources.[2–6] Recently, renewable energy sources have gained extraordinary attention due to their semi-infinitely renewable nature as well as their excellent energy harvesting efficiencies. Moreover, according to a 2024 report by the International Energy Agency (IEA), energy generation from renewable energy has rapidly increased over the past decade and is expected to overtake coal-based energy generation by the year 2025.[7] Nonetheless, there still remain many challenges to be addressed in order to completely remove reliance on fossil fuel and fulfill the Paris Agreement.

Solar energy is a carbon-free and renewable energy source where sunlight is harvested and converted into electric energy. Among many solar photovoltaic (PV) materials, metal halide perovskites of the ABX_3 structure (where A^+ = methylammonium (MA^+), formamidinium (FA^+), Cs^+, *etc.*, B^{2+} = Pb^{2+}, Sn^{2+}, *etc.*, X = I^-, Br^-, Cl^-, *etc.*) have recently stood out as a promising candidate ever since the first report by Kojima *et al.* in 2009.[8] Over the past 15 years, perovskite solar cells (PSCs) have reached 26.7% in power conversion efficiency (PCE) for single junction cells, comparable to the decades of progress by currently commercialized crystalline silicon.[9] Such outstanding performance is mostly enabled due to the excellent optoelectronic properties inherent to the perovskite material, such as a high absorption coefficient throughout the UV-vis-IR spectra, simple band gap tunability, ambipolar characteristics and long charge carrier diffusion lengths.[10–14] Throughout the development of PSCs, most researchers have primarily focused on the fabrication of PSCs through cost-efficient solution processing methods, largely due to the ease of fabrication and control over processing parameters.[15,16] Spin coating has been the go-to method for a majority of studies as it can result in ultra-thin polycrystalline perovskite films, and the involvement of antisolvents has assisted in greatly improving the surface morphology.[17] On the other hand, spin-coating is not suitable for fabricating larger devices, so other methods such as spray-pyrolysis, slot-die coating, blade coating and ink-jet printing have also been thoroughly explored.[13,18–24]

Despite the recent success of solution processed PSCs, most solvents used in perovskite precursors and anti-solvents used during fabrication are notorious for their toxicity. For example, dimethylformamide (DMF) is not only the most prevalent polar aprotic solvent used to dissolve the perovskite precursors, but also a commonly recognized carcinogen.[25,26] Anti-solvents such

Department of Chemical and Biological Engineering, Korea University, Seoul, 02841, Republic of Korea. E-mail: live2000jin@gmail.com, imromy@korea.ac.kr
† These authors contributed equally to this work.

as diethyl ether (DE), chlorobenzene (CB) and toluene (TOL) are also known for their toxicity as well as their hazardous nature particularly due to their volatile or flammable nature. Moreover, CB is also widely employed in the fabrication of charge transport layers (CTLs) such as 2,2′,7,7′-tetrakis[*N*,*N*-di(4-methoxyphenyl)amino]-9,9′-spirobifluorene (Spiro-OMeTAD) and phenyl-C61-butyric acid methyl ester (PCBM), which are essential for highly efficient PSCs.[27–29] Overall, while PSC commercialization is an attractive solution for carbon-free energy generation, the challenge of replacing hazardous solvents with ''green'' alternatives must be fully addressed.

Recently, researchers have actively sought for green alternatives that can also replicate the high efficiency of PSCs. The goal of this article is to summarize recent efforts for shifting towards fully green-processed efficient PSCs, including but not limited to the processing of perovskite layers and CTLs. Problems of the current state of solvents are first addressed, as well as an overall look into green alternatives and their selection criteria. A more comprehensive discussion on solvents used for the functional layer is then presented. Afterwards, a brief discussion on other green methods of PSC fabrication is given, followed by a short summary and perspectives on further challenges to be met in order to inspire the reader with a general direction to contribute towards carbon neutrality.

2. Solvents

2.1. Solvent selection considerations

The typical fabrication procedure of PSCs follows the deposition of the bottom CTL, the photo-active perovskite layer, and then the top CTL, sequentially on the transparent conductive electrode (TCE) substrate and the counter electrode on top. Here, the working solvents for solution processes are carefully selected in key consideration of (i) solvation capability, (ii) orthogonal processability, and (iii) the resulting film quality. The solvation capability of the solvent with respect to the precursor material, without the emergence of the undesired byproducts, is the primary criterion as it determines the viability of the solution process and the carrier potential of the solutes at an appropriate concentration. Moreover, the orthogonal processability is an indispensable factor in preparing vertically stacked heterojunctions through a solution process, as the working solvents should have negligible impact on the pre-formed underlying layer to achieve the discrete interfaces. Such a factor should account for the solubility of both the underlying material and the deposition material, favoring the latter while uninfluential to the former. Finally, the resulting film quality, such as the film morphology and the crystallinity, is significantly dependent on the physical properties and the chemical interactions between the precursor and the processing solvent. Various parameters for physical properties, including the boiling point, vapor pressure, surface tension, and viscosity, and for chemical interactions, including Hansen–Hildebrand solubility parameters, dielectric constants, polarity, proticity, Gutmann acceptor and donor numbers, and Kamlet–Taft solvent parameters, are simultaneously adopted to predict and engineer the above criteria for the optimal solution processing. Such features have been successfully achieved through implementing mixtures of solvents in complementary purposes compatible with the proposed solution-process-based deposition techniques, and the established solvents during the research stage of PSC fabrication are summarized in Table 1.

2.2 Solvent hazard considerations

While the feasible solution processibility of PSCs is advantageous for broad dissemination of renewable energy supply, it is necessary for the processing solvents to be safe in handling and treating to maintain a healthy and sustainable environment. However, currently many of the common solvents implemented in PSC development are accused of being highly toxic and detrimental to the environment, and thus hold limitations for future commercial applications. Accordingly, the development of green and less toxic solvents applicable to PSC fabrication is emphasized by the research and industrial community.[30–34]

The Safety, Health, and Environment (SH&E) criteria proposed by the CHEM21, which concords with the Global Harmonized System (GHS) and European regulations, provide effective solvent selection guidelines through various perspectives of the hazards associated with the solvent.[35,36] The SH&E classifies the solvent hazards into three categories: safety risk

Table 1 Summary of common processing solvents in perovskite research and their physical properties

Solvent	CAS number	T_{BP} (°C)	Viscosity (mPa s)	Vapor pressure (kPa)	Surface tension (mN m^{-1})	D_N (kcal mol^{-1})	Dielectric constant	δ_d (cal mL^{-1})$^{0.5}$	δ_p (cal mL^{-1})$^{0.5}$	δ_h (cal mL^{-1})$^{0.5}$
N,*N*-dimethylformamide (DMF)	68-12-2	153	0.92	0.36	36.76	26.6	36.71	8.5	6.7	5.5
Dimethyl sulfoxide (DMSO)	67-68-5	189	2.24	0.08	43.70	29.8	46.68	9.0	8.0	5.0
N-methyl-2-pyrrolidone (NMP)	872-50-4	202	1.67	0.05	40.70	27.3	32.20	8.8	6.0	3.5
γ-Butyrolactone (GBL)	96-48-0	204	1.73	1.50	35.40	18.0	40.96	9.3	8.1	3.6
Acetonitrile (ACN)	75-05-8	82	0.38	11.87	19.10	14.1	37.50	7.5	8.8	3.0
2-Methoxyethanol	109-86-4	124	1.72	0.82	31.80	19.8	16.93	7.9	4.5	8.0
Isopropanol (IPA)	67-63-0	82	2.37	4.30	21.79	21.1	19.92	7.7	3.0	8.0
Ethanol	64-17-5	78	1.14	5.87	22.32	19.2	24.55	7.7	4.3	9.5
Toluene (TOL)	108-88-3	92	0.59	3.87	28.53	0.1	2.38	8.8	0.7	1.0
Chlorobenzene (CB)	108-90-7	132	0.80	1.20	33.28	3.3	5.62	9.3	2.1	1.0
Diethyl ether (DE)	60-29-7	35	0.24	58.93	17.06	19.2	4.33	7.1	1.4	2.5
Water	7732-18-5	100	1.00	2.40	72.75	54.8	80.10	7.6	7.8	20.7

for workplace accidents at the production site associated with flammability and explosive accidents, health risk for occupational hazards associated with both acute and chronic health hazards such as irritations, intoxications, fertility issues, and carcinogenic, and finally environmental impacts during fabrication and demanding waste treatments which would cause environmental pollutions. Thus, the SH&E system comprehensively evaluates both the industrial application risks by probing safety and health hazards during the fabrication procedure and the following environmental impacts that may arise from implementing the processing solvents. The SH&E system classifies such hazardous risks from physical properties and health reports and labels the working solvents into ''recommended,'' ''problematic,'' and ''hazardous'' solvents, providing a suitable selection guide for the green and sustainable solvent replacements for the PSC preparation. The evaluation and classification of the common perovskite processing solvents by the SH&E criteria are listed in Table 2, along with the possible and studied replacement solvents for the greener and less toxic options for PSC development.

3. Green processing of the perovskite layer

3.1. Green solvents for perovskite precursors

The development of perovskite solar cells has been achieved through meticulous and continuous optimization with the initially established solvents. Due to the primary objective on the performance of the perovskite solar cells, safety concerns have often been overlooked, and there has been a lack of efforts to resolve the processing hazards. However, with the imminent practical application of perovskite solar cells, the processing solvents for fabricating perovskite solar cells should be compatible with industrial applications in terms of sustainability and availability. Meanwhile, alternatively developed solvents should not comprise efficiency despite their apparent advantages in benign environmental impact. In this review paper, we highlight studies that provide alternative processing routes for fabricating perovskite solar cells with comparable performance from alternative replacements for hazardous solvents.

Solution processing has consistently been the most reliable method to produce highly efficient PSCs compared to other

Table 2 Safety, Health and Environment (SH&E) evaluation of common solvents and the researched alternative solvents for perovskite solar cell preparation

Name	Safety	Health	Environment	Classification (primary hazard remarks)
Common solvents				
DMF	3	9	5	Hazardous (reproductive toxicity: H360D)
DMSO	1	1	5	Recommended
NMP	1	9	7	Hazardous (reproductive toxicity: H360D)
GBL	1	2	7	Problematic
can	4	3	3	Recommended
2-Methoxyethanol	3	9	3	Hazardous (reproductive toxicity: H360FD organ toxicity: H370)
IPA	4	3	3	Recommended
Ethanol	4	3	3	Recommended
TOL	5	6	3	Problematic
CB	3	2	7	Problematic
DE	10	3	7	Hazardous (high flammability: H224)
Water	1	1	1	Recommended
Alternative solvents				
2-Methylpyrazine	3	2	3	Recommended
Diethyl carbonate	3	2	3	Recommended
EA	5	3	3	Recommended
Isopropyl acetate	4	2	3	Recommended
2-MA	3	1	5	Recommended
3-MC	3	2	5	Recommended
Tetraethyl orthocarbonate	3	2	5	Recommended
Propylene carbonate	1	2	7	Problematic
N-formylmorpholine	1	2	7	Problematic
δ-Valerolactone	3	4	7	Problematic
GVL	1	5	7	Problematic
TEP	1	6	7	Problematic
Anisole	4	1	5	Problematic
Dibutyl ether	5	2	5	Problematic
Salicylaldehyde	1	6	5	Problematic
Methyl benzoate	1	6	5	Problematic
Acetic acid	3	7	3	Problematic
Benzoic acid	1	6	7	Problematic
Dimethyl sulfide	7	5	7	Hazardous (high flammability: H225)
Petroleum ether	7	2	7	Hazardous (high flammability: H224)
N,*N*-dimethylacetamide	1	9	5	Hazardous (reproductive toxicity: H360D)
Diisopropyl ether	9	3	5	Hazardous (high flammability: H225)
2,2,2-Trifluoroethanol	3	10	3	Hazardous (reproductive toxicity: H360F)

methods such as thermal co-evaporation.[37] Among countless reports, polar aprotic solvents such as DMF, dimethyl sulfoxide (DMSO) and *N*-methyl-2-pyrrolidone (NMP) have been the most widely used choices because they can effectively dissolve the perovskite precursors.[38] However, due to the known toxicity of these solvents as mentioned above, there have been extensive efforts to find green alternatives.[25,38–40] A good solvent for perovskite precursors should be able to dissolve the perovskite precursors consisting of alkyl halides and metal halides, and thus an aprotic polar solvent is highly desired. An effective strategy has been to screen for solvents with strong Lewis acid or base characteristics, as determined by the Gutmann donor number (D_N).[41,42] A popular green candidate has been γ-butyrolactone (GBL) with a D_N of 18 kcal mol^{-1}, which is sufficient to dissolve the perovskite precursors.[43–45] In 2020, Kim *et al.* used GBL as the sole solvent to process $MAPbI_{3-x}Cl_x$ perovskite thin films through ultrasonic spray coating.[44] Through careful optimization of the processing parameters, the GBL-based solution yielded a void-free perovskite thin film for the fabrication of PSCs with a best PCE of 17.14%. However, despite being less toxic than DMF, GBL in the human body can metabolically convert to γ-hydroxybutyric acid, which is an abused drug with adverse effects.[46,47]

In 2021, Worsley *et al.* demonstrated using a nontoxic and biodegradable alternative to GBL by using γ-valerolactone (GVL) as the only solvent for $AVA_{0.3}$–$MAPbI_3$ perovskite precursor solution (AVA = 5-aminovaleric acid).[48] The authors noted that while the optimized GVL-processed PSCs exhibited better performance (PCE = 12.91%) than the GBL-processed PSCs (PCE = 11.67%) and superior stability as shown in Fig. 1(a), the GVL-processed perovskite films were also subjective large voids resulting from fast crystallization. Miao *et al.* suggested that the strong interaction between GVL and the FA^+ can contribute towards obtaining a phase-pure α-$FAPbI_3$ film that remains stable for 60 days, as opposed to the DMF:DMSO-processed film that degrades after 7 days.[49] Compared to the 23.48% PCE of the DMF:DMSO-processed PSCs, the GVL-processed PSCs showed a much higher PCE of 25.09%. Meanwhile, a shortcoming of using GVL is the poor solubility of perovskite precursors due to the relatively low D_N of GVL. To overcome this problem, Kim *et al.* found that the presence of MACl within the precursor solution could increase the strength of

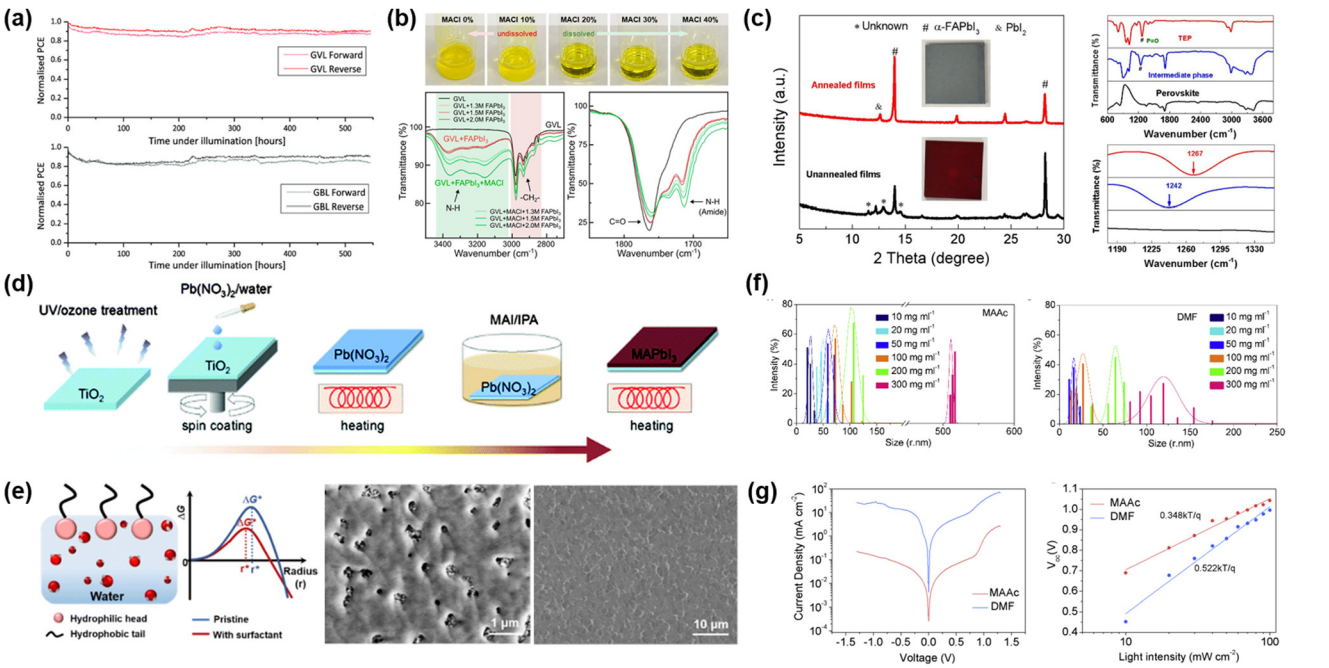

Fig. 1 (a) PCE stability comparison between PSCs processed from GVL (top) and GBL (bottom) (reproduced with permission from *Energy Technology*, 2021, **9**, 2100312. Copyright 2021 John Wiley & Sons, Inc.). (b) Changes in the solubility of GVL-based perovskite precursor solution with respect to MACl additive concentration, and Fourier transform infrared (FT-IR) spectra of the solutions showing the good interaction between the GVL-based solution and MACl (reproduced with permission from *ACS Sustainable Chemistry & Engineering*, 2024, **12**, 13371–13381. Copyright 2024 American Chemical Society). (c) X-ray diffraction (XRD) patterns and photo images of $FAPbI_3$ films fabricated from a TEP-based solution (left) and FT-IR spectra demonstrating the good interaction between the perovskite precursors and TEP in order to form a PbI_2–FAI–TEP adduct (reproduced with permission from *Chemical Engineering Journal*, 2022, **437**, 135458. Copyright 2022 Elsevier B.V.). (d) Schematic of the fabrication of perovskite films based on a non-toxic aqueous solution (reproduced with permission from *Chemical Communications*, 2015, **51**, 13294–13297. Copyright The Royal Society of Chemistry 2015). (e) Schematic of the addition of a surfactant (potassium oleate) to decrease the nucleation energy barrier of the aqueous $Pb(NO_3)_2$ solution (right) and the scanning electron microscopy (SEM) images comparing the $Pb(NO_3)_2$ film without (middle) and with (right) addition of the surfactant (reproduced with permission from *Energy & Environmental Science*, 2024, **17**, 296–306. Copyright The Royal Society of Chemistry 2024). (f) Dynamic light scattering (DLS) plots of the MAAc-based (left) and DMF-based (right) perovskite precursor solutions at varying concentrations and (g) comparison of dark current density levels (left) and the light intensity modulated V_{OC} (right) between the MAAc-based and DMF-based PSCs (reproduced with permission from *Chem*, 2019, **5**, 995–1006. Copyright 2019 Elsevier B.V.).

coordination between the solvent and lead halide ions, thus greatly increasing the solubility as shown in Fig. 1(b).[32] This was crucial for fabricating uniform perovskite films with large grains, and the PSCs with 40% MACl addition resulted in a best PCE of 20.59%. Interestingly enough, it happened to be the case that Miao *et al.* also incorporated MACl additives in order to fabricate a thick and uniform perovskite film.[49]

Triethyl phosphate (TEP) is another popular green candidate to replace DMF for green processing of the perovskite layer. TEP is often studied as a green solvent in membrane manufacturing that can replace polar solvents such as DMF and NMP.[50–55] Additionally, TEP and DMF have similar D_N values of 26 and 26.6 kcal mol^{-1}, respectively, indicating that TEP can be as good a solvent for the perovskite precursors as DMF.[50] One of the earliest applications of TEP in perovskite layer fabrication was reported by Cao *et al.* in 2022, where an $(FAPbI_3)_{0.95}$-$(MAPbBr_3)_{0.05}$ precursor solution in TEP was prepared with a concentration of 1.56 M.[51] The authors noted that TEP can interact well with the precursors through a Lewis acid–base reaction, forming a PbI_2–FAI–TEP adduct, as evidenced in Fig. 1(c), that results in a high quality perovskite layer with excellent morphology. The resulting PSCs had a best PCE of 20.13%. Cao *et al.* later showed that the TEP-based perovskite formation is also a stable process under high-humidity conditions, where the best PSC device exhibited a PCE of 19.86%.[52] This signifies that not only TEP is a suitable green alternative to DMF, but it can also free manufacturing design limitations due to its good ambient stability. Furthermore, in 2023, Wu *et al.* also demonstrated the use of TEP as the only solvent for the $(FAPbI_3)_{0.95}(MAPbBr_3)_{0.05}$ precursor and reported a high PCE of 22.42%.[53] Altogether, TEP is considered an excellent option for green chemistry in the fabrication of PSCs.

Water has also been actively explored as a potential solvent as it is one of the most environmentally friendly solvents as opposed to the toxic organic solvents, as well as one of the most abundant solvents available.[56–60] However, there is an obvious challenge as lead halide, one of the main perovskite precursors, is insoluble in water. To circumvent this, in 2015, Hsieh *et al.* first demonstrated an aqueous precursor solution of $Pb(NO_3)_2$ to replace the commonly used PbI_2 and DMF solution.[56] The proposed mechanism involves a two-step reaction where the $Pb(NO_3)_2$ film quickly reacts with MAI to form PbI_2, which then slowly reacts with excess MAI to form an $MAPbI_3$ film, as shown in Fig. 1(d). However, the best PCE of the resulting PSC device was low at 12.58%, mostly due to the poor perovskite morphology originating from the island-like deposition of $Pb(NO_3)_2$. Recently, many attempts afterwards have been made to resolve this issue and have been quite successful. Zhai *et al.* used a light modulation strategy during the two reactions to accelerate the formation of the PbI_2 and perovskite phases, and achieved a best performing PCE of 23.74%.[57] Soon afterwards, the same group further improved the PbI_2 layer formation process by replacing the $Pb(NO_3)_2$ precursor solution with $PbCO_3$ nanofluids, yielding a higher PCE of 24.16%.[58] Most recently, Zhang *et al.* recognized the high surface tension of water as the main cause of the island-like morphology of the $Pb(NO_3)_2$ layer and added potassium oleate as a surfactant to increase the $Pb(NO_3)_2$ nucleation rate, successfully fabricating a dense film from an aqueous $Pb(NO_3)_2$ solution as shown in Fig. 1(e).[59] They demonstrated a best PCE of 24.14% of the $FA_{1-x}M_xAPbI_{3-y}Cl_y$ PSC, which also showed excellent unencapsulated stability under harsh conditions.

Another problem that emerges with the various green solvents mentioned above is that most of the time the processing window for fabricating a defect-free perovskite film is very narrow. For instance, the use of GVL and TEP is often accompanied by the introduction of an antisolvent such as DE, TOL and CB. This has shifted the focus of many scientists towards ionic liquids as a green solvent for perovskite precursor solutions.[61–65] Ionic liquids are molten salts in a liquid state at room temperature that are usually highly viscous, non-volatile, hydrophobic and thermally stable, all of which make ionic liquids an attractive candidate for green chemistry.[61] A pioneer study by Moore *et al.* in 2015 revealed the possibility of using methylammonium formate as the solvent for the fabrication of an $MAPbI_3$ film.[62] This had then opened up many avenues for the study of PSC fabrication *via* ionic liquids. In 2019, Chao *et al.* used methylammonium acetate (MAAc), a room-temperature ionic liquid, as the solvent for the $MAPbI_3$ precursor solution, which was then used to fabricate PSCs with an impressive PCE of 20.05%.[63] The authors noted that the MAAc-based solution consisted of a highly uniform distribution of crystal nuclei compared to the relatively broad and uneven distribution in the DMF-based solution, as shown in Fig. 1(f), thus having a parallel effect on the crystal grain distribution of the resultant perovskite film. As a result, the MAAc-based PSCs had lower defect densities than the DMF-based PSCs as evidenced by the comparison of dark current levels and light intensity modulated open-circuit voltage (V_{OC}) measurements in Fig. 1(g). In 2021, Fang *et al.* also demonstrated using MAAc as the solvent for the $GA_{0.12}MA_{0.88}PbI_3$ perovskite solution (where GA^+ = guanidinium ion) and demonstrated a high PCE of 20.21%.[64] In particular, the authors used the highly viscous nature of MAAc to their advantage to blade-coat the perovskite films with relaxed strain and large grains. In 2022, Gu *et al.* reported that methylammonium propionate (MAP) can be used to fabricate higher quality perovskite films, which was then further evidenced by the PSCs with a high PCE of 20.56%.[65] Besides MAAc and MAP, there are still many variants of ionic liquids yet to be tested as green alternatives to DMF.

3.2. Green anti-solvents

Throughout the history of PSC fabrication, anti-solvent dripping has been a core strategy to produce perovskite thin films with full coverage and uniform morphology.[17] Typically, during the spin-coating process of a perovskite film, an 'anti-solvent' to the perovskite precursors will be dropped just as nucleation occurs in the wet film, effectively ''freezing'' the wet film at its intermediate state, which will then undergo crystal growth through solvent removal (such as heat treatment) in order to yield a dense and uniform thin film. However, the most commonly used anti-solvents such as DE and CB are not

environmental and health friendly. Moreover, the inherent nature of anti-solvent engineering involves a large volume of the toxic and volatile substance filling up the vicinity atmosphere, making it more of a concern. For these reasons, toxic anti-solvents have been primary targets to replace in order to establish green processes of PSC fabrication.[30,66–77]

An effective anti-solvent must be largely nonpolar such that it does not interact with the perovskite precursors, while possessing some degrees of polarity in order to be miscible with the solvents for the perovskite solution, as noticed by Bu *et al.* in 2017.[30] The authors classified many solvents by their polarity, boiling points and toxicity as shown in Fig. 2(a). Here, the ethylene acetate (EA) anti-solvent was found to be more effective than CB in forming a pinhole-free perovskite film, as shown in the bottom scheme of Fig. 2(a), and the EA-based PSCs exhibited a high PCE of 19.43%. Further investigation into the role of EA was performed by Xiang *et al.* in 2023.[71] Here, the effectiveness of EA as an anti-solvent was shown as less volume was required to precipitate the perovskite precursor solution compared to CB as shown in the photo images at the top left corner of Fig. 2(c). The quasi-2D Dion–Jacobson perovskite films prepared from EA treatment showed a much more uniform phase distribution than the CB-based films as shown in the transient absorption (TA) spectra in Fig. 2(c), which resulted in not only a higher PCE of 18.86% for the full device, but also better stability measured according to the ISOS-D-3 standards (damp heat conditions) and ISOS-L-1 standards (standard illumination conditions).

Another popular candidate for green anti-solvents is anisole (or methoxybenzene) due to its structural and characteristic similarity to another popular toxic anti-solvent, toluene. In 2018, Zhang *et al.* made comparisons between using CB and anisole as an anti-solvent for perovskite film fabrication and showed that the anisole-processed film exhibited larger grains and a smoother film morphology as shown in Fig. 2(b).[67] The anisole-based PSC demonstrated a high PCE of 19.42%, thus showing promise as a viable green antisolvent. Since then, many recent reports have started to use anisole as an effective anti-solvent.[68–70]

However, due to the inevitable nature of anti-solvents of which the purpose is to quickly extract precursor solvents and vaporize without affecting the perovskite film, it may be desirable to choose substances that are much more environmentally friendly and pose no risk to the environment at all. With this in mind, there have also been numerous studies exploring the effectiveness of alcohols as anti-solvents.[72–74] Chalkias *et al.* recently explored in depth the effects of different alcohols as anti-solvents on perovskite layer formation.[73] Compared to the commonly used CB anti-solvent, options such as methanol and ethanol are not as effective due to their higher polarity, which would consequently degrade the perovskite layer as shown by the XRD patterns and SEM images in Fig. 2(d). Meanwhile, as the alkyl chain length increases, the polarity of the alcohol decreases, and Chalkias *et al.* achieved a high PCE of 20.09% for $MAPbI_3$ PSCs when using 2-butanol. On the other hand, in order to compensate for the rather disruptive nature of ethanol on the perovskite layer, Xu *et al.* added MABr additives to the ethanol anti-solvent, which would then passivate the decomposed perovskite surface defects and enhance the film crystallinity.[72] This strategy not only yielded a high PCE of 21.53% for $Cs_{0.15}FA_{0.85}PbI_3$ PSCs, but also greatly enhanced the storage and operational stability of the final devices.

3.3. Green processes in perovskite crystallite synthesis

Perovskite reaction synthesis is another procedure requiring solvent processing, which synthesizes perovskite solute crystallites from separate lead salt and A-site cation salt.[78–86] The preparation procedures embody material purification, which removes detrimental impurities during the reaction process and allows the preparation of precursor materials in a stoichiometric balance with reduced defects.[82,87–91] Therefore, the perovskite solar cells fabricated from the crystallite precursors exhibit enhanced photovoltaic performance and superior reproducibility. Such a process necessitates a large mass of solvents, and thus there have been several attempts to derive synthesis methods using greener solvents.

A simple perovskite powder synthesis method was proposed by Heo *et al.* in 2016, from a solid–liquid reaction involving isopropanol as a green processing solvent.[78] As shown in Fig. 3(a), the solubilized A-site organic cation salt was left to react with the insoluble lead halide salt in the isopropanol (IPA) medium, leading to the successful preparation of $MAPbI_{3-x}Cl_x$ powders. Zhang *et al.* then demonstrated another solid–liquid preparation method to synthesize δ-$FAPbI_3$ using acetonitrile (ACN) as a green reaction medium in 2019.[92] Similarly, Mandal *et al.* reported on the synthesis methods using ACN as an antisolvent in combination with triethyl phosphate solubilized medium to prepare single-crystalline δ-$FAPbI_3$ through an antisolvent-assisted crystallization method, as presented in Fig. 3(b).[93] The ACN acted as an effective antisolvent inducing crystallization of the perovskite crystallites compared to other non-polar solvent alternatives, leading to high-quality and large-size crystals with suppressed defects in high yield. Recently, Nambiraj *et al.* reported a series of perovskite material perovskite preparation methods using GVL solvent as a less-toxic alternative.[94] The inverse temperature crystallization technique, which can be seen in Fig. 3(c), was implemented to synthesize δ-$FAPbI_3$ microcrystals by continuously heating the homogenized solution containing perovskite precursors, leading to precipitation. Moreover, Pan *et al.* demonstrated a synthesis method for preparing δ-$FAPbI_3$ powders with water as a processing solvent containing hydriodic acid as a simultaneous solubilizing agent and a halide supply.[95] As depicted in Fig. 3(d), the acid-assisted solubilized lead iodide salt is reacted with the FA^+ cation by incorporating formamidinium acetate (FAAc) salt, leading to the precipitation of δ-$FAPbI_3$ powders. The above-described methods overall present a simple and greener choice for preparing perovskite precursors.

3.4. Summary

It goes without saying that a good quality perovskite layer is crucial to fabricate highly performing PSCs. Therefore, when considering a greener and sustainable approach to the

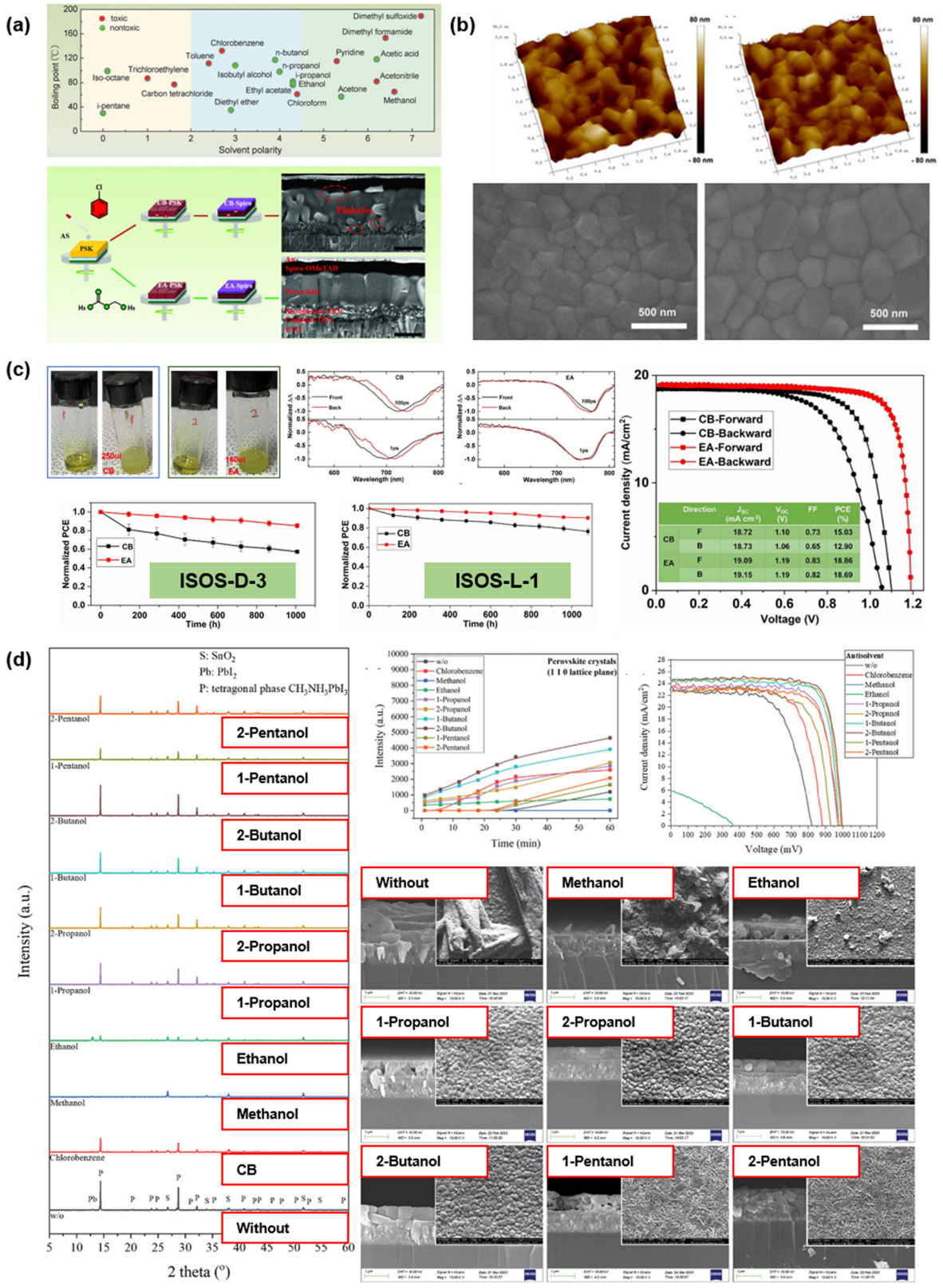

Fig. 2 (a) Classification of various solvents by their boiling point, polarity and toxicity (top) and comparative scheme between using the conventional CB and the non-toxic EA as the anti-solvent for perovskite film formation (bottom) (reproduced with permission from *Advanced Energy Materials*, 2017, **7**, 1700576. Copyright 2017 John Wiley & Sons, Inc.). (b) Atomic force microscopy (AFM) images (top row) and SEM images (bottom row) of the perovskite film surface fabricated from CB (left) and anisole (right) anti-solvent processing (reproduced with permission from *Solar RRL*, 2018, **2**, 1700213. Copyright 2018 John Wiley & Sons, Inc.). (c) Photos of turbid perovskite solutions with the addition of different amounts of CB (left) and EA (right) anti-solvents (top left), TA spectrum comparison of perovskite films prepared from CB and EA (top middle), current density–voltage (*J*–*V*) curves of CB-based and

EA-based PSC devices (right), and ISOS-standardized stability tests of the PSC devices under damp heat (left) and standard illumination (right) conditions (bottom row) (reproduced with permission from *Chemical Engineering Journal*, 2023, **460**, 141758. Copyright 2023 Elsevier B.V.). (d) XRD patterns (left) and time evolution of the (110) peaks (top middle) of perovskite films prepared from various alcohols as anti-solvents, SEM images of the corresponding perovskite films (bottom), and *J*–*V* curves of their final PSC devices (top right) (reproduced with permission from *Advanced Functional Materials*, 2024, **34**, 2406354. Copyright 2024 John Wiley & Sons, Inc.).

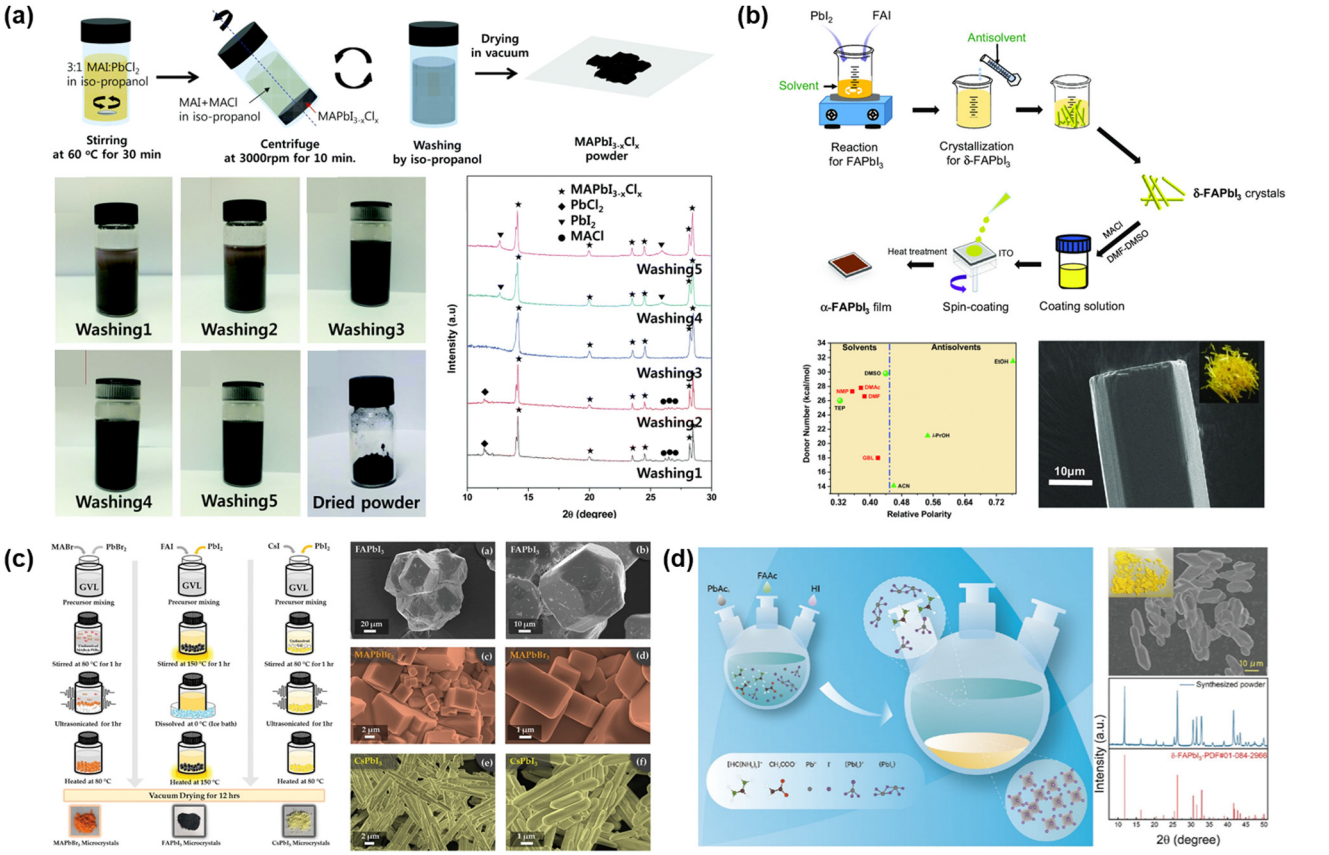

Fig. 3 The schematic illustration and their resultant perovskite crystal precursors with (a) IPA (Reproduced with permission from *Nanoscale*, 2016, **8**, 2554–2560. Copyright The Royal Society of Chemistry 2016.) (b) TEP and ACN (Reproduced with permission from *Solar RRL*, 2023, **7**, 2300496. Copyright 2023 John Wiley & Sons, Inc.) (c) GVL (Reproduced with permission from *Small Methods*, 2024, 2400768 (early view). Copyright 2024 John Wiley & Sons, Inc.) and (d) water (Reproduced with permission from *Science China Materials*, 2024, **67**, 1621–1630. Copyright 2024 Springer Nature.) as green processing solvents.

development of PSCs, it makes sense to first ensure that the alternative green solvents are highly suitable for the fabrication of a high-quality perovskite thin film. This section has showcased the numerous and innovative attempts at achieving green fabrication of the perovskite light harvesting layer, including – but not limited to – green solvents for the perovskite precursor solution (GVL, TEP and water), non-toxic anti-solvents (anisole, EA, and alcohols), and green processes for the synthesis of high purity perovskite crystallites. A summary of green solvents for perovskite precursor solutions and their respective device performances can be found in Table 3, and a summary of green anti-solvents and their respective device performances can be found in Table 4.

4. Green solvents for the CTLs

When discussing the green chemistry of PSC fabrication, discussion on the fabrication of the CTLs is usually inevitable. Almost all high-performing PSC devices consist of two separate CTLs – a hole transporting layer (HTL) and an electron transporting layer (ETL) – sandwiching the intrinsic perovskite layer. Because of this, most CTLs are either processed by non-polar solvents in order to avoid damaging the underlying perovskite layer, or designed such that they will not be affected by the polar perovskite solution. Some of the most commonly used non-polar solvents are TOL and CB, which possess alarming degrees of toxicity either to the environment or to the health of its handler or, in some cases, both, as mentioned in Table 2.[99,100]

4.1. Green processing of HTLs

Most PSCs with the highest reporting PCEs recently have been based on the n–i–p structure, employing Spiro-OMeTAD as the HTL.[9] However, Spiro-OMeTAD is usually dissolved in CB for processing, which poses many hazardous threats due to its volatility, flammability, ability to react with the ozone layer of the atmosphere, and tendency to degrade into other harmful

Table 3 List of studies replacing toxic perovskite precursor solvents with non-toxic green solvents

Year	Device structure	Green solvent	Replacement	J_{SC} [mA cm^{-2}]	V_{OC} [V]	FF [%]	PCE [%]	Ref.
2015	FTO/TiO_2/mp-TiO_2/$MAPbI_3$/Spiro-OMeTAD/Au	Water/IPA	DMF	21.81	0.94	61	12.58	56
2019	ITO/CPTA/BACl/$MAPbI_3$/Spiro-OMeTAD/MoO_3/Au	MAAc	DMF, DMSO, NMP, GBL, DMAc	23.16	1.11	78.01	20.05	63
2020	FTO/TiO_2/mp-TiO_2/$MAPbI_{3-x}Cl_x$/PTAA/Au	GBL	DMF	21.55	1.08	73.64	17.14	44
2021	FTO/TiO_2/(mp-TiO_2/$AVA_{0.3}$-$MAPbI_3$/ZrO_2)/carbon	GVL	GBL, DMF:DMSO	23.42	0.9	61	12.91	48
2021	PET/IZO/PEDOT:PSS/$Cs_{0.1}(FA_{0.83}MA_{0.17})_{0.9}$-$Pb(I_{0.83}Br_{0.17})_3$/$C_{60}$/BCP/Ag	GBL/2MP	DMF	19.00	1	69.2	11.4	43
2021	FTO/SnO_2/$GA_{0.12}MA_{0.88}PbI_3$/Spiro-OMeTAD/Au	MAAc	DMF, GBL	22.66	1.17	76.37	20.21	64
2022	FTO/SnO_2/$(FAPbI_3)_{0.95}(MAPbBr_3)_{0.05}$/PEAI/Spiro-OMeTAD/Au	TEP	DMF	24.69	1.09	74.8	20.13	51
2022	FTO/TiO_2/mp-TiO_2/$MAPbI_3$/Spiro-OMeTAD/Ag	ACN	DMF:DMSO	25.13	1.05	77.01	20.3	117
2022	FTO/TiO_2/$CsPbBr_3$/carbon	Water/EGME	MeOH	7.48	1.51	84.49	9.55	60
2022	FTO/TiO_2/mp-TiO_2/(FA,MA)$PbI_{3-x}Cl_x$/PEAI/Spiro-OMeTAD/Au	Water/IPA	DMF	24.94	1.187	80.2	23.74	57
2022	ITO/SnO_2/$MAPbI_3$/Spiro-OMeTAD/MoO_3/Ag	MAP	DMF	23.39	1.12	78.48	20.56	65
2023	FTO/TiO_2/SnO_2/$FAPbI_3$/TBMAI/Spiro-OMeTAD/Ag	GVL	DMF:DMSO	25.91	1.165	83.1	25.09	49
2023	FTO/SnO_2/$(FAPbI_3)_{0.95}(MAPbBr_3)_{0.05}$/PEAI/Spiro-OMeTAD/Au	TEP	DMF	24.13	1.085	72.6	19	54
2023	ITO/SnO_2/$FAPbI_3$/Spiro-OMeTAD/Au	TEP	DMF, HI, DMAc, NMP, GBL	24.62	1.16	79.18	22.61	93
2023	FTO/SnO_2-NRs/$(FAPbI_3)_{0.95}(MAPbBr_3)_{0.05}$/Spiro-OMeTAD/Ag	TEP	DMF	24.6	1.12	81.36	22.42	53
2023	FTO/TiO_2/mp-TiO_2/(FA,MA)$PbI_{3-x}Cl_x$/OAI/Spiro-OMeTAD/Au	Water/IPA	DMF	24.95	1.178	82.2	24.16	58
2024	ITO/SnO_2/$FAPbI_3$/Spiro-OMeTAD/Au	GVL	DMF, NMP, DMAc	23.8	1.12	77.47	20.59	32
2024	FTO/TiO_2/mp-TiO_2/(FA,MA)$Pb(I,Cl)_3$/OAI/Spiro-OMeTAD/metal electrode[a]	Water	DMF	25.24	1.172	81.6	24.14	59
2024	ITO/PTAA/PFN-Br/$BA_2FA_3Pb_4I_{13}$/PCBM/BCP/Ag	TEP	DMF	23.34	1.03	72.5	17.42	55
2024	ITO/PTAA/$FA_{0.2}MA_{0.8}PbI_3$-SC:CTAC/C_{60}/BCP/Cu	GBL	DMF	25.2	1.1	84.4	23.4	45
2024	FTO/SnO_2/$(FAPbI_3)_{0.95}(MAPbBr_3)_{0.05}$/PEAI/Spiro-OMeTAD/Au	TEP	DMF	23.46	1.105	76.6	19.86	52

[a] Type of metal electrode was not specified.List of abbreviations: mp-TiO_2 = mesoporous TiO_2; IPA = 2-propanol; DMF = *N*,*N*-dimethylformamide; CPTA = C_{60} pyrrolidine tris-acid; BACl = butylammonium chloride; MAAc = methylammonium acetate; DMSO = dimethyl sulfoxide; NMP = *N*-methyl-2-pyrrolidone; GBL = γ-butyrolactone; DMAc = dimethylacetamide; AVA = 5-aminovaleric acid; GVL = γ-valerolactone; BCP = bathocuproine; 2MP = 2-methylpyrazine; GA = guanidinium; PEAI = phenylethylammonium iodide; TEP = triethyl phosphate; ACN = acetonitrile; EGME = ethylene glycol monomethyl ether; MeOH = methanol; MAP = methylammonium propionate; TBMAI = tributylmethylammonium iodide; HI = hydriodic acid; NRs = nanorods; OAI = octylammonium iodide; BA = butylammonium; SC = single crystal; CTAC = hexadecyltrimethylammonium chloride.

chlorinated chemicals.[99,101] In search of a green alternative, scientists have opted to choose one of the following two strategies: find a new green solvent to replace CB, or design a new hole transporting material that is soluble in known green non-polar solvents.[98,102–108]

A simpler strategy for green processing of HTLs in n–i–p devices is to find an alternative solvent that could well solubilize Spiro-OMeTAD while not damaging the perovskite layer. For example, in 2019, Jiang *et al.* used tetrahydrofuran (THF), instead of CB, as a non-halogenated green solvent to process the HTL.[102] According to the authors, using THF held multiple advantages of CB, apart from being a greener alternative, such as creating a more crystalline HTL so that no hygroscopic doping is required. However, while the THF-based device showed an improved PCE of 16.96% compared to the 15.27% PCE of the CB-based device, it is worth noting that the volatile nature of THF still calls for caution by the handler. Another candidate to replace CB was explored by Cao *et al.* as they used anisole to dissolve and process Spiro-OMeTAD, yielding a high PCE of 19.0%.[54] Most recently, Guo *et al.* used EA and demonstrated that it held multiple advantages over CB as evidenced by the excellent PCE of the EA-based PSCs at 23.3%.[103] Not only is EA a green solvent with little health or environmental hazards, but the authors show that the stereo-chemistry of EA allows it to more readily oxidize Spiro-OMeTAD due to its stronger electropositivity compared to CB as shown in Fig. 4(a).

Meanwhile, other researchers have instead chosen to focus on synthesizing new p-type compounds that can readily dissolve in verified green solvents.[98,104–107] In 2017, Lee *et al.* synthesized a donor–acceptor (D–A) type polymer-like HTM consisting of benzothiadiazole (BT) and benzo[1,2-*b*:4,5:*b*′]dithiophene (BDT), which could be solubilized by the green solvent 2-methyl-anisole (2-MA).[104] Reporting a PCE of 20.0%, this was one of the first ever reports to synthesize a hole conducting polymer tailored to be processed by 2-MA. The same group later designed a different D–A type polymer named alkoxy-PTEG, which is based on a similar backbone as the previously synthesized polymer, but with a tetraethylene glycol-substituted BT and alkoxy groups replacing the BDT groups so that the new polymer is more soluble in non-aromatic solvents such as 3-methylcyclohexanone (3-MC).[105] This change arose from the concern that solvents with aromatic benzene rings such as 2-MA may still pose health risks. The newly fabricated PSC with the 3-MC processed HTL showed a high PCE of 19.9% and also proved to be able to be processed just as well by other solvents such as CB and 2-MA.

Table 4 List of studies replacing toxic perovskite anti-solvents with non-toxic green anti-solvents

Year	Device structure	Green solvent	Replacement	J_{SC} [mA cm^{-2}]	V_{OC} [V]	FF [%]	PCE [%]	Ref.
2017	FTO/TiO_2/$FA_{0.85}MA_{0.15}Pb(I_{0.85}Br_{0.15})_3$/Spiro-OMeTAD/Au	EA	CB	22.89	1.123	75.6	19.43	30
2018	FTO/TiO_2/$Cs_{0.05}(FA_{0.83}MA_{0.17})_{0.95}Pb(I_{0.83}Br_{0.17})_3$/ Spiro-OMeTAD/Au	PhOMe	CB	22.78	1.1	77.52	19.42	67
2020	ITO/PTAA/$Cs_{0.15}FA_{0.85}PbI_3$/PCBM/Phen-NADPO/Ag	EtOH	CB, Tol	25.07	1.09	78.79	21.53	72
2020	FTO/SnO_2/$MAPbI_3$/Spiro-OMeTAD/Au	EA	CB	21.44	1.115	74.58	17.83	75
2020	ITO/NiO_x/$MAPbI_3$/PCBM/BCP/Ag	TEOC	CB	21.9	1.06	78	18.15	97
2022	FTO/SnO_2/$(FAPbI_3)_{0.95}(MAPbBr_3)_{0.05}$/ PEAI/Spiro-OMeTAD/Au	DBE	CB	24.69	1.09	74.8	20.13	51
2022	ITO/SnO_2/$MAPbI_3$/Spiro-OMeTAD/Au	IPA:TPAI	Tol	23.004	1.122	79	20.4	74
2022	FTO/TiO_2/$MAPbI_3$/Spiro-OMeTAD/Au	EA:AA	CB	24.48	1.12	76.95	21.09	66
2022	ITO/FMPA-BT-CA/$FA_{0.15}MA_{0.85}PbI_{0.9}Cl_{0.1}$/$C_{60}$/BCP/Cu	EA	CB	23.33	1.151	83.3	22.37	98
2023	FTO/TiO_2/SnO_2/$FAPbI_3$/TBMAI/Spiro-OMeTAD/Ag	BAc	CB, DE	25.91	1.165	83.1	25.09	49
2023	ITO/SnO_2/$FAPbI_3$/Spiro-OMeTAD/Au	SAL:PEAI	DE, IPA	25.1	1.02	79	20.23	76
2023	FTO/SnO_2/$(FAPbI_3)_{0.95}(MAPbBr_3)_{0.05}$/ PEAI/Spiro-OMeTAD/Au	DBE	CB	24.13	1.085	72.6	19	54
2023	ITO/SnO_2/$FAPbI_3$/Spiro-OMeTAD/Au	ACN	DE	24.62	1.16	79.18	22.61	93
2023	ITO/PTAA/$FAPbI_3$/C_{60}/BCP/Ag	ACN	DE, CF, MeOH, EtOH	24.42	1.17	82.19	23.48	79
2023	ITO/PEDOT:PSS/$FASnI_3$/C_{60}/BCP/Cu	DEC	CB, Tol	24.2	0.8	73.5	14.2	77
2023	FTO/TiO_2/(DMePDA)$FA_3Pb_4I_{13}$/Spiro-OMeTAD/Au	EA	CB	19.09	1.19	83	18.86	71
2024	ITO/PTAA/PFN-Br/$BA_2FA_3Pb_4I_{13}$/PCBM/BCP/Ag	PE	CB	23.34	1.03	72.5	17.42	55
2024	PEN/ITO/SnO_2/$MAPbI_3$/PEDOT:PSS/carbon	2-BA	CB	24.6	0.996	82	20.09	73

List of abbreviations: EA = ethyl acetate; CB = chlorobenzene; PhOMe = methoxybenzene; Phen-NADPO = 3-[6-(diphenylphosphinyl)-2-naphthalenyl]-1,10-phenanthroline; Tol = toluene; TEOC = tetraethyl orthocarbonate; DBE = dibutyl ether; TPAI = tryptaminium iodide; AA = acetylacetone; FMPA-BT-CA = [fluorinated-(methoxy-substituted triphenylamine)]-[benzo[*c*][1,2,5]thiadiazole]-[cyanoacetic acid]; BAc = *n*-butyl acetate; DE = diethyl ether; SAL = salicylaldehyde; CF = chloroform; DEC = diethyl carbonate; DMePDA = *N*,*N*-dimethyl-1,3-propanediamine; PE = petroleum ether; 2-BA = 2-butanol.

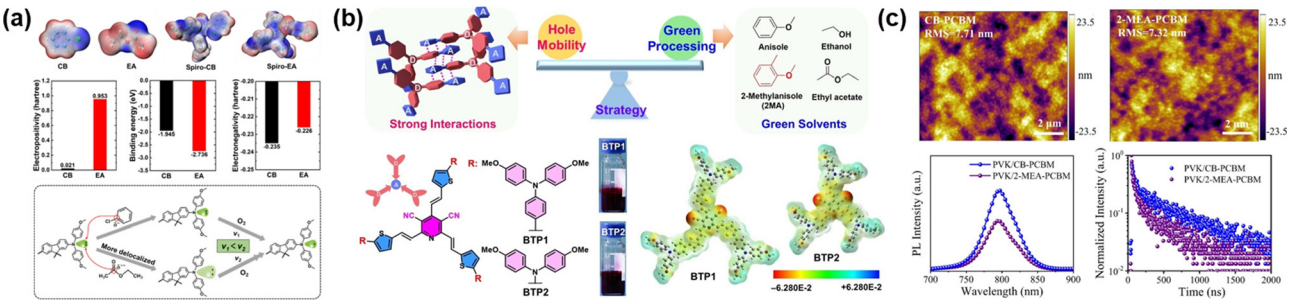

Fig. 4 (a) Comparison of properties between CB-based and EA-based Spiro-OMeTAD solutions and their reaction pathways (reproduced with permission from *Solar RRL*, 2024, **8**, 2300934. Copyright 2024 John Wiley & Sons, Inc.). (b) Schematic representation of BTP1 and BTP2 as new D–A–D type hole transporting materials (reproduced with permission from *Angewandte Chemie*, 2023, **135**, e202218752. Copyright 2023 John Wiley & Sons, Inc.). (c) AFM image comparison between PCBM films processed with CB (top left) and 2-MA (top right), and the PL (bottom left) and TRPL (bottom right) spectra of the two films (reproduced with permission from *ACS Applied Materials & Interfaces*, 2022, **15**, 1042–1052. Copyright 2022 American Chemical Society).

Similarly, new green solvent-processable HTLs were designed to be used in p–i–n type PSCs as well. In 2022, Liao *et al.* designed a D–A type molecule consisting of fluorinated methoxy-substituted triphenylamine (MPA), BT and cyanoacetic acid (CA), hence referred to as FMPA–BT–CA.[98] The newly synthesized FMPA–BT–CA was dissolved in IPA and spun into a thin film on the TCE substrate. The final PSC device showed an excellent PCE of 22.37%, which was the highest at the time for PSCs with green solvent processed HTMs. Recently in 2023, Yu *et al.* synthesized two new star-shaped compounds of a D–A–D structure, which they deemed to be an effective structure for hole transport.[107] The two compounds, each named BTP1 and BTP2, can be visualized in Fig. 4(b). In particular, BTP1 was processed using the green solvent 2-MA and coated on the TCE substrate to be built into a p–i–n type PSC, which subsequently demonstrated an outstanding PCE of 24.32%. However, there are noticeably fewer reports on designing HTMs for p–i–n type PSCs as opposed to the n–i–p-type PSCs. This likely stems from the fact that inorganic HTMs such as metal oxides can be used as the bottom layer for inverted structures. Such metal oxides (*i.e.* NiO_x) are typically aqueously processed, negating the need to search for green alternatives in the first place.

4.2. Green processing of ETLs

Most reports of ETLs used in n–i–p devices are metal oxides such as SnO_2, TiO_2 and ZnO, which are prepared in either aqueous solutions or alcohol solutions, and hence they do not

Table 5 List of studies replacing toxic charge transport layer precursor solvents with non-toxic green solvents

Year	Target	Device structure	Green solvent	Replacement	J_{SC} [mA cm^{-2}]	V_{OC} [V]	FF [%]	PCE [%]	Ref.
2017	HTL	FTO/TiO_2/$FA_{0.85}MA_{0.15}Pb(I_{0.85}Br_{0.15})_3$/Spiro-OMeTAD/Au	EA	CB	22.89	1.123	75.6	19.43	30
2017	HTL	FTO/TiO_2/mp-TiO_2/$Cs_{0.05}(FA_{0.85}MA_{0.15})Pb(I_{0.85}Br_{0.15})_3$/asy-PBTBDT/Au	2-MA	CB, DCB, Tol	22.8	1.12	79.4	20	104
2019	HTL	ITO/C_{60}/$MAPbI_{3-x}Cl_x$/Spiro-OMeTAD/MoO_3/Ag	THF	CB	21.29	1.023	77.78	16.94	102
2020	HTL	FTO/SnO_2/$Cs_{0.06}FA_{0.78}MA_{0.16}Pb_{0.94}I_{2.4}Br_{0.48}$/alkoxy-PTEG/Au	2-MA	CB	23.2	1.14	79.8	21.2	105
2020	HTL	FTO/SnO_2/$Cs_{0.06}FA_{0.78}MA_{0.16}Pb_{0.94}I_{2.4}Br_{0.48}$/alkoxy-PTEG/Au	3-MC	CB, 2-MA	23.3	1.13	75.7	19.9	105
2020	HTL	ITO/C_{60}/$MAPbI_{0.9}Cl_{0.1}$/F23/MoO_3/Ag	THF	CB	21.62	1.07	76.08	17.6	108
2021	HTL	FTO/SnO_2/$GA_{0.12}MA_{0.88}PbI_3$/Spiro-OMeTAD/Au	EA	CB	22.66	1.17	76.37	20.21	64
2023	HTL	ITO/SnO_2/$FAPbI_3$/BDT-C8-3O/MoO_3/Au	3-MC	CB	25.39	1.16	79.87	23.53	98
2023	HTL	FTO/SnO_2/$(FAPbI_3)_{0.95}(MAPbBr_3)_{0.05}$/PEAI/Spiro-OMeTAD/Au	Anisole	CB	24.13	1.085	72.6	19	106
2023	HTL	ITO/SnO_2/$FA_xMA_{1-x}PbI_3$/PEAI/Spiro-OMeTAD/MoO_3/Ag	EA	CB	24.1	1.16	83.7	23.3	54
2022	HTL	ITO/FMPA-BT-CA/$FA_{0.15}MA_{0.85}PbI_{0.9}Cl_{0.1}$/$C_{60}$/BCP/Cu	IPA	CB, CF	23.33	1.151	83.3	22.37	103
2023	HTL	ITO/BTP1/$Cs_{0.05}(FA_{0.98}MA_{0.02})Pb(I_{0.98}Br_{0.02})_3$/PEACl/$C_{60}$/BCP/Ag	2-MA	CB	24.95	1.178	82.83	24.34	107
2020	ETL	ITO/NiO_x/$MAPbI_3$/PCBM/BCP/Ag	Anisole	CB	21.9	1.06	78	18.15	97
2023	ETL	PET/ITO/NiO_x/$Cs_{0.05}(FA_{0.98}MA_{0.02})Pb(I_{0.98}Br_{0.02})_3$/PCBM/BCP/Ag	2-MA:DIO	CB	22.72	1.096	81.51	20.3	109

List of abbreviations: asy = asymmetric; 2-MA = 2-methyl-anisole; DCB = dichlorobenzene; THF = tetrahydrofuran; 3-MC = 3-methylcyclohexanone; BDT = benzodithiophene; PEACl = phenylethylammonium chloride; DIO = 1,8-diiodooctane.

pose much risks to the surrounding environment. On the other hand, for p–i–n type devices, ETLs such as PCBM are solution-processed on top of the perovskite layer, where the toxic solvent CB is used. Therefore, developing green processing methods for the solution-processed ETLs on a perovskite film has been addressed as well.[97,109] In 2020, Wang *et al.* used anisole to process PCBM on a perovskite film and found that the anisole-based solution could produce a much smoother PCBM film compared to the CB-based solution.[97] They posited that the anisole molecules could form stronger electrostatic interactions with the PCBM molecules because of the $-OCH_3$ group, while the aromatic ring of anisole could also better interact with the C_{60} groups than CB could. Similarly, in a recent study by Ma *et al.*, a comparison between n–i–p type PSC devices with CB-processed and 2-MA-processed PCBM layers was made.[109] As shown in Fig. 4(c), Ma *et al.* also reported a smoother PCBM film when using 2-MA as the solvent in contrast to using CB. This also promoted more efficient charge transfer from the perovskite to the ETL, as shown in the PL and TRPL plots in Fig. 4(c), thus demonstrating a high PCE of 20.30%.

4.3. Green processing at perovskite/CTL interfaces

Besides the fabrication of perovskite and CTL layers, treatment at their interfaces is also extremely important for achieving high-performing PSCs.[96,110] Interface engineering usually takes the form of solution processing at their respective surfaces, and thus it is also important to consider the environmental and safety implications of these processes. In large, interface engineering can be classified by whether it is processed on the buried interface or the top perovskite/CTL interface. Some of the most popular forms of buried interface modification use ionic salts or carboxylate salts that can form good interactions with either the bottom CTL, which are usually metal oxides, or the perovskite layer.[111–114] Meanwhile, most reported cases of top perovskite/CTL interface treatment employ alkylammonium halide salts for passivation and band structure modification of the perovskite surface.[58,59,115,116] In either case, interface engineering usually uses water for the treatment of ionic or carboxylate salts, or IPA for the treatment of ammonium halides, which are already non-hazardous solvents. Therefore, in a green solvent processing perspective, it appears that perovskite/CTL interface treatment poses minimal trouble.

4.4. Summary

Solvents used in the fabrication of charge transport layers are also concerns for achieving sustainable development of PSCs, especially considering that there are two different layers to be processed for each device. However, the selection criteria for CTLs, the top layer in particular, are slightly more restrictive since any solvent that may decompose the underlying perovskite layer cannot be used. In search of a greener fabrication of CTLs, scientists have mainly focused on two strategies: (1) find a suitable replacement to the toxic non-polar organic solvent, CB, which is most commonly used; and (2) design a new organic charge transporting material that is solution processable in already-known green solvents such as 2-MA and 3-MC. While many studies have emerged for green fabrication of HTLs, there have been comparatively fewer reports on the green fabrication of ETLs such as PCBM, which could be due to the fact that many studies have chosen to use a vacuum evaporated C_{60} layer as the top ETL instead. A summary of green solvents used for the processing of CTLs can be found in Table 5.

5. Scalable fabrication using green solvents

Recent transition towards green solvent-based PSCs has also motivated scientists to actively demonstrate integration into scalable production such as large-area modules of PSCs. While

spin-coating has always been the most popular method of thin-film fabrication for small area devices, its effectiveness decreases in terms of uniformity as the substrate area increases and is also notorious for its wasteful nature of solvents and precursors, particularly when anti-solvent dripping is also involved. As a result, many have opted for more solvent-efficient methods of large-scale PSC fabrication, such as solution shearing, blade coating, ink-jet printing for thin-film fabrication, and bathing for anti-solvent treatment.[49,117–123]

Solvent properties are crucial towards achieving high quality large-area perovskite thin films. Availability becomes much narrower when simultaneously considering the green nature of solvents. A popular choice of green solvent for large-area perovskite film fabrication has been ACN. In 2022, Adugna *et al.* demonstrated solution-shearing of large-area perovskite thin films using an ACN/methylamine (MA) solvent system.[117] By creating a viscous gel of MA-absorbed $MAPbI_3$ and mixing it with ACN, the authors were able to develop and optimize a solution-sheared perovskite thin film that was uniform over a large 10 × 10 cm^2 area. However, they only fabricated small area devices albeit with a high PCE of 20.3%. Most recently, Duan *et al.* recognized the shortcomings of ACN as a replacement for DMF, being that the lower D_N of ACN (14.1 kcal mol^{-1}) resulted in weaker coordination with the Pb^{2+} ions within the perovskite precursor, causing the formation of $[PbX_m]^{2-m}$ complexes (m = 0–6), which is unfavorable for high quality perovskite films.[119] To compensate, small amounts of ethanol (EtOH) with a high acceptor number (37.9 kcal mol^{-1}) were added to the DMSO/ACN solvent mixture in order inhibit this process and enhance the crystallinity of the perovskite film. The authors noted that the high volatility of ACN and EtOH (compared to that of DMSO) was also beneficial in controlling the crystallization process at low temperatures. Ultimately, the authors demonstrated a large-area (20.25 cm^2) all-perovskite tandem module with a high PCE of 22.2%. Meanwhile, Chalkias *et al.* used a GVL-based perovskite solution for inkjet-printing of the $MAPbI_3$ layer.[120] By also inkjet-printing the ETLs, disregarding the HTL, and screen-printing the carbon electrode, the authors successfully demonstrated an HTL-free, all-green processed, scalable perovskite mini-module on a 10 × 10 cm^2 substrate with a PCE of 10.07% (active area = 52.5 cm^2).

Despite the above advances, there still remains much to explore in green-solvent-based scalable PSCs. ACN by itself is not suitable for the aforementioned scalable methods such as shearing, blade-printing and slot-die coating due to its low viscosity, D_N and other solvent properties. Other solvents such as GVL and TEP may offer improvements in this regard, but few have been reported as of yet. In addition, the scalable fabrication of other green-solvent-based layers (*i.e.* HTLs, ETLs) has yet to be explored. For example, Cheng *et al.* demonstrated a 5 × 5 cm^2 PSC mini-module using BDT-DC8-3O as the HTL, which used 3-MC as the green solvent.[106] The mini-module exhibited a high PCE of 20.04% with an active area of 15.64 cm^2. Zhai *et al.* also fabricated a 6 × 6 cm^2 PSC mini-module using D-OC6 as the HTL and 2-MA as the green solvent.[124] This device showed a high PCE of 21% based on an active area of 17.1 cm^2. However, both examples employed spin-coating of the green-solvent-based HTL, which might pose difficulties for

Table 6 List of studies employing green solvents for scalable fabrication of perovskite solar cells and/or modules

Year	Target	Method	Green solvent	Replacement	Area [cm^2]	PCE [%]	Notes	Ref.
2022	Perovskite	Shear	ACN/MA	DMF, DMSO	0.04	20.3	10 × 10 cm^2 large area shear coating for perovskite films only. Device performance for a small area only (0.04 cm^2)	117
2023	Perovskite	Blade	ACN	DMF, DMSO		20.05	No large area modules or perovskite films. A blade coated unit cell provides future opportunities for scalability	118
2023	Perovskite		GBL:MSM	DMF, DMSO	25	19.9	7 × 7 cm^2 mini-module. Does not specify method for large area perovskite layer fabrication	123
2023	Perovskite	Inkjet	GVL	DMF	52.4	10.07	10 × 10 cm^2 mini-module. All layers up to the perovskite are fabricated *via* inkjet printing	120
2024	Perovskite	Blade	ACN/EtOH/ DMSO	DMF	0.049	19	Small area, but with blade coating of green solvent. WBG perovskite (later used in Tandem module)	119
2024	Perovskite	Blade	ACN/EtOH/ DMSO	DMF	0.049	19.6	Small area, but with blade coating of green solvent. NBG perovskite (later used in Tandem module)	119
2024	Perovskite	Blade	ACN/EtOH/ DMSO	DMF	20.25	22.2	6 × 6 cm^2 All-perovskite tandem module. All green solvent processed for both WBG and NBG perovskite layers	119
2019	Antisolvent	Bath	*n*-BuOH	CB, DE	53.46	13.85	10 × 10 cm^2 mini-module	121
2020	Antisolvent	Bath	FACl/2-PeOH	DE	1	18.08	5 × 5 cm^2 large area fabrication on the perovskite film only. The largest device area was 1.00 cm^2	122
2023	Antisolvent	Bath	BAc	CB, DE	61.6	20.46	10 × 10 cm^2 mini-module. Perovskite layer was spin coated, and then bathed by BAc anti-solvent	49
2023	Antisolvent	Bath	BAc	CB	25	19.9	7 × 7 cm^2 mini-module	123
2023	HTL	Spin	3-MC	CB	15.64	20.04	5 × 5 cm^2 mini-module	106
2023	HTL	Spin	2-MA	CB	17.1	21	6 × 6 cm^2 mini-module	124

List of abbreviations: MA = methylamine; MSM = methylsulfonylmethane; *n*-BuOH = *n*-butanol; 2-PeOH = 2-pentanol.

larger modules. Overall, there still remains a large room for development on scalable green processing of perovskite solar cells or modules, and a summary on its recent progress is provided in Table 6.

6. Summary and perspectives

The rapid progress that perovskite PVs have shown over the past decade has been more than enough to captivate countless scientists in a world of possibilities that perovskite solar cells have to offer in the future. However, with such amazing scientific progress, a certain degree of caution must also be taken by carefully and thoroughly considering possible consequences in the case of negligence. As perovskite solar cells have approached closer to commercialization, their impact on the environment and the health of their manufacturers has also been recognized as an unavoidable challenge to be met. As it has been discussed numerous times throughout this article, the solution processability of perovskite solar cells appears to be a double-edged sword; while the solution processing technology can offer a wide range of techniques for the fabrication of highly efficient solar cells, careful analysis and selection of the solvents and techniques must be performed to avoid undesired hazards.

As it stands now, many of the most effective methods reported to fabricate perovskite solar cells are still strongly dependent on toxic and hazardous solvents such as DMF, DE, CB and TOL. Selection of green alternatives to such solvents has been the primary theme around which this article has revolved. Green solvents such as GVL, TEP, water, ionic liquids, alcohols and ACN have been investigated to replace DMF as the perovskite precursor solvent. Extensive research on green anti-solvents has been performed, such as EA and anisole for replacing DE and CB. Green solvents such as 2-MA and 3-MC for the fabrication of charge transport layers have been considered in conjunction with the development of new materials that are more suitable with such green solvents. However, there remains some debate regarding whether a solvent is truly ''green'' compared to other candidates within that category. Among the many prolific reports on ''green solvents'', we believe that the perovskite solar cell research community would greatly benefit from an establishment of common standards for green-processed and sustainable development of perovskite solar cells.

Finally, the proceeding step would be to reduce the required amount of the replaced solvents for efficient management of resources and minimizing risks. As briefly discussed above, development of large-scale production techniques with lower solution consumption would facilitate both the practicality of perovskite solar cells and a greener fabrication environment. For instance, meniscus-based deposition methods such as slot-die, bar coating, blade coating, ink-jet printing and spray-deposition methods have been viable techniques for fabricating large-area perovskite solar modules while minimizing solvent consumption, as opposed to the solvent-wasteful spin-coating techniques demonstrated in popular literature. In continuation to the search of green solvents, their integration into the above solvent-efficient techniques would further enable fully-green fabrication processes of perovskite solar cells.

Data availability

No primary research results, software or code have been included and no new data were generated or analysed as part of this review.

Conflicts of interest

There are no conflicts to declare.

Acknowledgements

This study was supported by the National Research Foundation of Korea (NRF) under the Ministry of Science, ICT & Future Planning (no. 2022R1C1C2008126, no. 2022R1A2C3004964, and no. 2024M3H4A1A03044871) and the Technology Innovation Program (20012770, High Permeability Thermoplastic Elastomer for Solar Module) funded by the Ministry of Trade, Industry & Energy (MOTIE, Korea).

Notes and references

1 The Paris Agreement, **https://unfccc.int/process-and-meetings/the-paris-agreement)**.
2 X. Tian, C. An and Z. Chen, *Renewable Sustainable Energy Rev.*, 2023, **182**, 113404.
3 R. Rohit, D. C. Kiplangat, R. Veena, R. Jose, A. Pradeepkumar and K. S. Kumar, *Renewable Sustainable Energy Rev.*, 2023, **184**, 113531.
4 J. Krūmiņš and M. Kļaviņš, *Energies*, 2023, **16**, 3612.
5 Z. Guzović, N. Duić, A. Piacentino, N. Markovska, B. V. Mathiesen and H. Lund, *Energy*, 2023, **263**, 125617.
6 F. J. Nijsse, J.-F. Mercure, N. Ameli, F. Larosa, S. Kothari, J. Rickman, P. Vercoulen and H. Pollitt, *Nat. Commun.*, 2023, **14**, 6542.
7 Electricity Mid-Year Update July 2024, **https://www.iea.org/reports/electricity-mid-year-update-july-2024)**.
8 A. Kojima, K. Teshima, Y. Shirai and T. Miyasaka, *J. Am. Chem. Soc.*, 2009, **131**, 6050–6051.
9 Best Research-Cell Efficiency Chart, **https://www.nrel.gov/pv/cell-efficiency.html)**.
10 J. H. Noh, S. H. Im, J. H. Heo, T. N. Mandal and S. I. Seok, *Nano Lett.*, 2013, **13**, 1764–1769.
11 S. D. Stranks, G. E. Eperon, G. Grancini, C. Menelaou, M. J. Alcocer, T. Leijtens, L. M. Herz, A. Petrozza and H. J. Snaith, *Science*, 2013, **342**, 341–344.
12 J. H. Heo, S. H. Im, J. H. Noh, T. N. Mandal, C.-S. Lim, J. A. Chang, Y. H. Lee, H.-J. Kim, A. Sarkar and M. K. Nazeeruddin, *Nat. Photonics*, 2013, **7**, 486–491.
13 J. H. Heo, F. Zhang, C. Xiao, S. J. Heo, J. K. Park, J. J. Berry, K. Zhu and S. H. Im, *Joule*, 2021, **5**, 481–494.
14 H. J. Lee, J. K. Park, D. S. Lee, S. Choi, S. Y. Hong, J. H. Heo and S. H. Im, *ACS Appl. Energy Mater.*, 2022, **5**, 3660–3667.
15 D. Liu and T. L. Kelly, *Nat. Photonics*, 2014, **8**, 133–138.
16 P. Wang, Y. Wu, B. Cai, Q. Ma, X. Zheng and W. H. Zhang, *Adv. Funct. Mater.*, 2019, **29**, 1807661.
17 N. J. Jeon, J. H. Noh, Y. C. Kim, W. S. Yang, S. Ryu and S. I. Seok, *Nat. Mater.*, 2014, **13**, 897–903.
18 D. S. Lee, M. J. Ki, H. J. Lee, J. K. Park, S. Y. Hong, B. W. Kim, J. H. Heo and S. H. Im, *ACS Appl. Mater. Interfaces*, 2022, **14**, 7926–7935.

19 J. K. Park, S. Y. Kim, J. H. Kim, J. H. Heo and S. H. Im, *J. Alloys Compd.*, 2022, **918**, 165560.
20 J. B. Whitaker, D. H. Kim, B. W. Larson, F. Zhang, J. J. Berry, M. F. Van Hest and K. Zhu, *Sustainable Energy Fuels*, 2018, **2**, 2442–2449.
21 Z. Yang, C. C. Chueh, F. Zuo, J. H. Kim, P. W. Liang and A. K. Y. Jen, *Adv. Energy Mater.*, 2015, **5**, 1500328.
22 X. Peng, J. Yuan, S. Shen, M. Gao, A. S. Chesman, H. Yin, J. Cheng, Q. Zhang and D. Angmo, *Adv. Funct. Mater.*, 2017, **27**, 1703704.
23 J. H. Heo, J. K. Park, H. J. Lee, E. H. Shin, S. Y. Hong, K. H. Hong, F. Zhang and S. H. Im, *Adv. Mater.*, 2024, 2408387.
24 J. K. Park, J. H. Heo, H. J. Lee, B. W. Kim, S. W. Park, K.-H. Hong and S. H. Im, *J. Alloys Compd.*, 2023, **965**, 171499.
25 N. Yang, X. Chen, F. Lin, Y. Ding, J. Zhao and S. Chen, *J. Hazard. Mater.*, 2014, **264**, 278–285.
26 V. Scailteur and R. Lauwerys, *Toxicology*, 1987, **43**, 231–238.
27 Y. Zhong, M. Hufnagel, M. Thelakkat, C. Li and S. Huettner, *Adv. Funct. Mater.*, 2020, **30**, 1908920.
28 N. J. Jeon, H. G. Lee, Y. C. Kim, J. Seo, J. H. Noh, J. Lee and S. I. Seok, *J. Am. Chem. Soc.*, 2014, **136**, 7837–7840.
29 H. J. Lee, J. K. Park, J. H. Heo and S. H. Im, *Energy Environ. Mater.*, 2024, **7**, e12582.
30 T. Bu, L. Wu, X. Liu, X. Yang, P. Zhou, X. Yu, T. Qin, J. Shi, S. Wang and S. Li, *Adv. Energy Mater.*, 2017, **7**, 1700576.
31 S. Shan, Y. Li, H. Wu, T. Chen, B. Niu, Y. Zhang, D. Wang, C. Kan, X. Yu and L. Zuo, *SusMat*, 2021, **1**, 537–544.
32 B. J. Kim, H. Choi, S. Park, M. B. Johansson, G. Boschloo and M.-C. Kim, *ACS Sustainable Chem. Eng.*, 2024, **12**, 13371–13381.
33 R. Vidal, J.-A. Alberola-Borràs, S. N. Habisreutinger, J.-L. Gimeno-Molina, D. T. Moore, T. H. Schloemer, I. Mora-Seró, J. J. Berry and J. M. Luther, *Nat. Sustainability*, 2021, **4**, 277–285.
34 K. L. Gardner, J. G. Tait, T. Merckx, W. Qiu, U. W. Paetzold, L. Kootstra, M. Jaysankar, R. Gehlhaar, D. Cheyns and P. Heremans, *Adv. Energy Mater.*, 2016, **6**, 1600386.
35 D. Prat, A. Wells, J. Hayler, H. Sneddon, C. R. McElroy, S. Abou-Shehada and P. J. Dunn, *Green Chem.*, 2016, **18**, 288–296.
36 F. P. Byrne, S. Jin, G. Paggiola, T. H. Petchey, J. H. Clark, T. J. Farmer, A. J. Hunt, C. Robert McElroy and J. Sherwood, *Sustainable Chem. Processes*, 2016, **4**, 1–24.
37 Y. Vaynzof, *Adv. Energy Mater.*, 2020, **10**, 2003073.
38 X. Cao, L. Zhi, Y. Jia, Y. Li, K. Zhao, X. Cui, L. Ci, D. Zhuang and J. Wei, *ACS Appl. Mater. Interfaces*, 2019, **11**, 7639–7654.
39 H. J. Beaulieu and K. R. Schmerber, *Appl. Occup. Environ. Hyg.*, 1991, **6**, 874–880.
40 M. Behrouzeh, M. Abbasi, S. Osfouri and M. J. Dianat, *J. Environ. Chem. Eng.*, 2020, **8**, 103597.
41 J. C. Hamill Jr, J. Schwartz and Y.-L. Loo, *ACS Energy Lett.*, 2017, **3**, 92–97.
42 V. Gutmann, *Electrochim. Acta*, 1976, **21**, 661–670.
43 B. Wilk, S. Oz, E. Radicchi, F. Unlu, T. Ahmad, A. P. Herman, F. Nunzi, S. Mathur, R. Kudrawiec and K. Wojciechowski, *ACS Sustainable Chem. Eng.*, 2021, **9**, 3920–3930.
44 S. S. Kim, J. H. Heo and S. H. Im, *RSC Adv.*, 2020, **10**, 33651–33661.
45 N. Liu, N. Li, C. Jiang, M. Lv, J. Wu and Z. Chen, *Angew. Chem., Int. Ed.*, 2024, **63**, e202314089.
46 R. B. Palmer, *Toxicol. Rev.*, 2004, **23**, 21–31.
47 D. M. Wood, A. D. Brailsford and P. I. Dargan, *Drug Test. Anal.*, 2011, **3**, 417–425.
48 C. Worsley, D. Raptis, S. Meroni, A. Doolin, R. Garcia-Rodriguez, M. Davies and T. Watson, *Energy Technol.*, 2021, **9**, 2100312.
49 Y. Miao, M. Ren, Y. Chen, H. Wang, H. Chen, X. Liu, T. Wang and Y. Zhao, *Nat. Sustainability*, 2023, **6**, 1465–1473.
50 J. Chang, J. Zuo, L. Zhang, G. S. O'Brien and T.-S. Chung, *J. Membr. Sci.*, 2017, **539**, 295–304.
51 X. Cao, L. Hao, Z. Liu, G. Su, X. He, Q. Zeng and J. Wei, *Chem. Eng. J.*, 2022, **437**, 135458.
52 X. Cao, G. Su, L. Hao, J. Zhou, Q. Zeng, X. He and J. Wei, *J. Mater. Chem. C*, 2024, **12**, 1631–1639.
53 X. Wu, Y. Zheng, J. Liang, Z. Zhang, C. Tian, Z. Zhang, Y. Hu, A. Sun, C. Wang and J. Wang, *Mater. Horiz.*, 2023, **10**, 122–135.
54 X. Cao, L. Hao, G. Su, X. Li, T. Dong, P. Chao, D. Mo, Q. Zeng, X. He and J. Wei, *RSC Sustainability*, 2023, **1**, 1290–1297.
55 G. Zhang, J. Tang, C. Wang, X. Wu, J. Chen, X. Wang, K. Wang, X. Zhu, H. Yu and J. Li, *Green Chem.*, 2024, **26**, 5347–5355.
56 T.-Y. Hsieh, T.-C. Wei, K.-L. Wu, M. Ikegami and T. Miyasaka, *Chem. Commun.*, 2015, **51**, 13294–13297.
57 P. Zhai, L. Ren, S. Li, L. Zhang, D. Li and S. F. Liu, *Matter*, 2022, **5**, 4450–4466.
58 P. Zhai, L. Ren, Y. Zhang, Z. Xu, Y. Wu, K. Zhao, L. Zhang and S. F. Liu, *Energy Environ. Sci.*, 2023, **16**, 3014–3024.
59 Y. Zhang, L. Ren, P. Zhai, J. Xin, J. Wu, Q. Zhang, X. Chen, K. Zhao, L. Zhang and S. F. Liu, *Energy Environ. Sci.*, 2024, **17**, 296–306.
60 S. Wang, F. Cao, W. Sun, C. Wang, Z. Yan, N. Wang, Z. Lan and J. Wu, *Mater. Today Phys.*, 2022, **22**, 100614.
61 J. Ma, L. Wang, K. He, Y. Sun, B. Li, Q. Zhao and B. Du, *J. Mater. Chem. C*, 2024, **12**, 10837–10856.
62 D. T. Moore, K. W. Tan, H. Sai, K. P. Barteau, U. Wiesner and L. A. Estroff, *Chem. Mater.*, 2015, **27**, 3197–3199.
63 L. Chao, Y. Xia, B. Li, G. Xing, Y. Chen and W. Huang, *Chem*, 2019, **5**, 995–1006.
64 J. Fang, Z. Ding, X. Chang, J. Lu, T. Yang, J. Wen, Y. Fan, Y. Zhang, T. Luo and Y. Chen, *J. Mater. Chem. A*, 2021, **9**, 13297–13305.
65 L. Gu, C. Ran, L. Chao, Y. Bao, W. Hui, Y. Wang, Y. Chen, X. Gao and L. Song, *ACS Appl. Mater. Interfaces*, 2022, **14**, 22870–22878.
66 J. Li, X. Hua, F. Gao, X. Ren, C. Zhang, Y. Han, Y. Li, B. Shi and S. F. Liu, *J. Energy Chem.*, 2022, **66**, 1–8.
67 M. Zhang, Z. Wang, B. Zhou, X. Jia, Q. Ma, N. Yuan, X. Zheng, J. Ding and W. H. Zhang, *Sol. RRL*, 2018, **2**, 1700213.
68 C. Li, L. Chen, F. Jiang, Z. Song, X. Wang, A. Balvanz, E. Ugur, Y. Liu, C. Liu and A. Maxwell, *Nat. Energy*, 2024, 1–9.
69 F. Jiang, Y. Shi, T. R. Rana, D. Morales, I. E. Gould, D. P. McCarthy, J. A. Smith, M. G. Christoforo, M. Y. Yaman and F. Mandani, *Nat. Energy*, 2024, 1–10.
70 W.-T. Wang, P. Holzhey, N. Zhou, Q. Zhang, S. Zhou, E. A. Duijnstee, K. J. Rietwyk, J.-Y. Lin, Y. Mu and Y. Zhang, *Nature*, 2024, **632**, 294–300.
71 J. Xiang, X. Li, S. Gong, S. Wang, X. Chen and F. Zhang, *Chem. Eng. J.*, 2023, **460**, 141758.
72 W. Xu, Y. Gao, W. Ming, F. He, J. Li, X. H. Zhu, F. Kang, J. Li and G. Wei, *Adv. Mater.*, 2020, **32**, 2003965.
73 D. A. Chalkias, A. Nikolakopoulou, L. C. Kontaxis, A. N. Kalarakis and E. Stathatos, *Adv. Funct. Mater.*, 2024, 2406354.
74 Y. Zhao, Y. Tan, L. Wan, L. Lou and Z.-S. Wang, *ACS Appl. Energy Mater.*, 2022, **5**, 9520–9529.
75 W. Zhang, Y. Li, X. Liu, D. Tang, X. Li and X. Yuan, *Chem. Eng. J.*, 2020, **379**, 122298.
76 J. Cho, B. Kim, S. Ryu, A. J. Yun, B. Gil, J. Lim, J. Kim, J. Kim and B. Park, *Electron. Mater. Lett.*, 2023, **19**, 462–470.
77 Z. Zhang, Y. Huang, C. Wang, Y. Jiang, J. Jin, J. Xu, Z. Li, Z. Su, Q. Zhou and J. Zhu, *Energy Environ. Sci.*, 2023, **16**, 3430–3440.
78 J. H. Heo and S. H. Im, *Nanoscale*, 2016, **8**, 2554–2560.
79 T. N. Mandal, J. H. Heo, S. H. Im and W. S. Kim, *Small*, 2023, **19**, 2305246.
80 S. W. Park, J. H. Heo, J. Lee, H. Kim, S. H. Im and K.-H. Hong, *ACS Energy Lett.*, 2023, **8**, 5061–5069.
81 P. Zhu, D. Wang, Y. Zhang, Z. Liang, J. Li, J. Zeng, J. Zhang, Y. Xu, S. Wu and Z. Liu, *Science*, 2024, **383**, 524–531.
82 H. Min, M. Kim, S.-U. Lee, H. Kim, G. Kim, K. Choi, J. H. Lee and S. I. Seok, *Science*, 2019, **366**, 749–753.
83 M. Kim, G.-H. Kim, T. K. Lee, I. W. Choi, H. W. Choi, Y. Jo, Y. J. Yoon, J. W. Kim, J. Lee and D. Huh, *Joule*, 2019, **3**, 2179–2192.
84 J. Jeong, M. Kim, J. Seo, H. Lu, P. Ahlawat, A. Mishra, Y. Yang, M. A. Hope, F. T. Eickemeyer and M. Kim, *Nature*, 2021, **592**, 381–385.
85 P. K. Nayak, D. T. Moore, B. Wenger, S. Nayak, A. A. Haghighirad, A. Fineberg, N. K. Noel, O. G. Reid, G. Rumbles and P. Kukura, *Nat. Commun.*, 2016, **7**, 13303.
86 Y. Wang, Z. Shi, Y. Wang, Q. U. Khan, X. Li, L. Deng, Y. Pan, X. Zhang, Y. Yang and X. Yue, *Adv. Mater.*, 2023, **35**, 2302298.
87 D.-h Song, J. H. Heo, H. J. Han, M. S. You and S. H. Im, *J. Power Sources*, 2016, **310**, 130–136.
88 Y. Zhang, T. Yang, S.-U. Lee, S. Liu, K. Zhao and N.-G. Park, *ACS Energy Lett.*, 2023, **9**, 159–167.
89 J. Yao, L. Yang, F. Cai, Y. Yan, R. S. Gurney, D. Liu and T. Wang, *Sustainable Energy Fuels*, 2018, **2**, 436–443.
90 S. J. Lee, J. H. Heo and S. H. Im, *ACS Appl. Mater. Interfaces*, 2020, **12**, 8233–8239.
91 M. Ozaki, A. Shimazaki, M. Jung, Y. Nakaike, N. Maruyama, S. Yakumaru, A. I. Rafieh, T. Sasamori, N. Tokitoh and P. Ekanayake, *Angew. Chem., Int. Ed.*, 2019, **58**, 9389–9393.

92 Y. Zhang, S. Seo, S. Y. Lim, Y. Kim, S.-G. Kim, D.-K. Lee, S.-H. Lee, H. Shin, H. Cheong and N.-G. Park, *ACS Energy Lett.*, 2019, **5**, 360–366.
93 T. N. Mandal, J. H. Heo, S. H. Im and W.-S. Kim, *Sol. RRL*, 2023, **7**, 2300496.
94 B. Nambiraj, A. Kunka Ravindran, S. P. Muthu and R. Perumalsamy, *Small Methods*, 2024, 2400768.
95 Y. Pan, Y. Wang, M. Deng, Q. Zeng, L. Li, X. Liao, M. Zhang, W. Wang, F. Xie and F. Liu, *Sci. China Mater.*, 2024, **67**, 1621–1630.
96 H. J. Lee, J. H. Heo and S. H. Im, *Appl. Phys. Rev.*, 2024, **11**, 031301.
97 M. Wang, Q. Fu, L. Yan, J. Huang, Q. Ma, M. Humayun, W. Pi, X. Chen, Z. Zheng and W. Luo, *Chem. Eng. J.*, 2020, **387**, 123966.
98 Q. Liao, Y. Wang, M. Hao, B. Li, K. Yang, X. Ji, Z. Wang, K. Wang, W. Chi and X. Guo, *ACS Appl. Mater. Interfaces*, 2022, **14**, 43547–43557.
99 C. Wang, J.-y Xi and H.-y Hu, *Chemosphere*, 2008, **73**, 1167–1171.
100 J. M. Donald, K. Hooper and C. Hopenhayn-Rich, *Environ. Health Perspect.*, 1991, **94**, 237–244.
101 T. Vysokikh, T. Yagodovskaya, S. Savilov and V. Lunin, *Russ. J. Phys. Chem. A*, 2007, **81**, 878–882.
102 K. Jiang, F. Wu, G. Zhang, L. Zhu and H. Yan, *Sol. RRL*, 2019, **3**, 1900061.
103 B. Guo, X. Chen, H. Luo, G. O. Odunmbaku, T. Jiang, N. A. N. Ouedraogo, Z. Huang, Q. Gao, B. Zhang and Y. Ouyang, *Sol. RRL*, 2024, **8**, 2300934.
104 J. Lee, M. Malekshahi Byranvand, G. Kang, S. Y. Son, S. Song, G.-W. Kim and T. Park, *J. Am. Chem. Soc.*, 2017, **139**, 12175–12181.
105 J. Lee, G. W. Kim, M. Kim, S. A. Park and T. Park, *Adv. Energy Mater.*, 2020, **10**, 1902662.
106 Q. Cheng, H. Chen, W. Chen, J. Ding, Z. Chen, Y. Shen, X. Wu, Y. Wu, Y. Li and Y. Li, *Angew. Chem., Int. Ed.*, 2023, **62**, e202312231.
107 X. Yu, D. Gao, Z. Li, X. Sun, B. Li, Z. Zhu and Z. A. Li, *Angew. Chem.*, 2023, **135**, e202218752.
108 H. Lu, B. He, Y. Ji, Y. Shan, C. Zhong, J. Xu, J. LiuYang, F. Wu and L. Zhu, *Chem. Eng. J.*, 2020, **385**, 123976.
109 X. Ma, J. Kong, W. Wang and X. Li, *ACS Appl. Mater. Interfaces*, 2022, **15**, 1042–1052.
110 Z. Ni, C. Bao, Y. Liu, Q. Jiang, W.-Q. Wu, S. Chen, X. Dai, B. Chen, B. Hartweg and Z. Yu, *Science*, 2020, **367**, 1352–1358.
111 X. Ji, L. Bi, Q. Fu, B. Li, J. Wang, S. Y. Jeong, K. Feng, S. Ma, Q. Liao and F. R. Lin, *Adv. Mater.*, 2023, **35**, 2303665.
112 P. Chen, W. Pan, S. Zhu, F. Cao, A. Tong, R. He, Z. Lan, W. Sun and J. Wu, *Chem. Eng. J.*, 2023, **468**, 143652.
113 Q. Sun, X. Meng, G. Liu, S. Duan, D. Hu, B. Shen, B. Kang and S. R. P. Silva, *Adv. Funct. Mater.*, 2024, **34**, 2404686.
114 Q. Li, H. Liu, C.-H. Hou, H. Yan, S. Li, P. Chen, H. Xu, W.-Y. Yu, Y. Zhao and Y. Sui, *Nat. Energy*, 2024, 1–11.
115 D. S. Lee, J. H. Heo, J. K. Park, B. W. Kim, H. J. Lee, Y. M. Song and S. H. Im, *ACS Appl. Mater. Interfaces*, 2021, **13**, 16775–16783.
116 J. H. Heo, F. Zhang, J. K. Park, H. J. Lee, D. S. Lee, S. J. Heo, J. M. Luther, J. J. Berry, K. Zhu and S. H. Im, *Joule*, 2022, **6**, 1672–1688.
117 G. B. Adugna, S. Y. Abate and Y.-T. Tao, *Chem. Eng. J.*, 2022, **437**, 135477.
118 P. Baral, X. Zhang, K. Garden, N. Chakraborty, L. Shen, Z. Cao, X. Gong, L. Whittaker-Brooks and H. Wang, *Org. Electron.*, 2023, **116**, 106763.
119 C. Duan, H. Gao, K. Xiao, V. Yeddu, B. Wang, R. Lin, H. Sun, P. Wu, Y. Ahmed and A. D. Bui, *Nat. Energy*, 2024, 1–11.
120 D. Chalkias, A. Mourtzikou, G. Katsagounos, A. Kalarakis and E. Stathatos, *Small Methods*, 2023, **7**, 2300664.
121 S. Tian, J. Li, S. Li, T. Bu, Y. Mo, S. Wang, W. Li and F. Huang, *Sol. Energy*, 2019, **183**, 386–391.
122 Y. Zhang, Y. Tu, X. Yang, R. Su, W. Yang, M. Yu, Y. Wang, W. Huang, Q. Gong and R. Zhu, *ACS Appl. Mater. Interfaces*, 2020, **12**, 24905–24912.
123 Y. Y. Kim, S. M. Bang, J. Im, G. Kim, J. J. Yoo, E. Y. Park, S. Song, N. J. Jeon and J. Seo, *Adv. Sci.*, 2023, **10**, 2300728.
124 M. Zhai, M. Li, Z. Deng, R. Yao, L. Wang, C. Chen, H. Wang, X. Ding, L. Liu and X. Li, *ACS Energy Lett.*, 2023, **8**, 4966–4975.